Malaysian Journal of Catalysis
http://mjcat.utm.my/
MJCat
Research Article

Experimental Study of The Pressure Drop Rotating and Flooding in A Packed Bed Reactor

Usman Garba[1,2*] David Rouzineau[1,] Michel Meyer[1]

[1]*Chemical Engineering Laboratory, University of Toulouse, CNRS, INPT, UPS, Toulouse, France*
[2]*Usmanu Danfodiyo University Sokoto, Nigeria*

**Corresponding Author: usman.garba@udusok.edu.ng*

Article history:
Received 01 November 2023
Accepted 11 December 2023

ABSTRACT

The almost zero sensitivity to variations in gravitational force offered by rotating packed bed (RPB) reactors as gas/liquid contactor for multi-phase catalytic reactions was explored. A pilot-scale RPB with a casing diameter of 0.676m, inner rotor diameter of 0.160m, and an outer rotor diameter of 0.500m equipped with a standard, multi-layered, stainless steel wire mesh packing of axial height 0.040m, a specific surface of 2400 m^2/m^3 and a porosity of 86% was used. The scarcity of fundamental data on the hydrodynamics and mass transfer of the reactor limits the design, scale-up, and retrofitting of RPB reactors. Hence, the focus was on the hydrodynamic behaviour of the device. Previous studies on RPB reactor flooding and operating limits dwelled on visual observations and pressure drop variations only. However, physical visualizations are subjective because pressure drop variations of RPB reactors are too inconsistent to be used in obtaining the upper operating limit during their operations. A robust quantitative method of obtaining RPB reactor flooding limits based on the flow rate of the ejected liquid, supported by visual observation and pressure drop measurement, was presented for a rotation speed range, gas flowrate and, liquid flowrate range of 0 -1500 rpm, 0 - 400 Nm^3h^{-1} and 0-0.84 m^3h^{-1} respectively. The aim was to identify, with greater certainty, RPB reactor hydrodynamic characteristics and provide a more standard method of identifying it. The average increase in single-phase pressure drops per unit increase in rotation speed and the average increase in pressure drop per unit increase in gas flow rate was 0.75Pa/rpm and 4.11Pa/m^3h^{-1} respectively. The upper operating limits found showed that to attain a particular capacity of RPB reactors at a given gas and liquid flowrates, a particular rotation speed is required which can simply be altered to vary the other operating parameters towards attaining stable operations.

Keywords: *Rotating packed bed reactor, Pressure drop, Flooding, Gas-liquid contactor, heterogeneous catalytic reactions*

| eISSN 0128-2581 |

1. INTRODUCTION

Reliance on gravitational force makes conventional packed columns for separation processes such as distillation and absorption have unimpressive sizes and physical footprints which makes them uneconomical, especially where space and weight are limited[1], [2]. The operating ranges of non-rotating, conventional, packed bed columns (PBCs) are limited by gravitational and frictional forces acting in opposite directions on the down-flowing liquid and the gas flowing from the bottom of the column. A RPB reactor, also called HIGEE (High g) contactor, is a compact process intensification equipment in which a combination of sizeable allowable gas and liquid flow rates is achieved by superimposing gravitational force with centrifugal force. In RPB reactors, the higher gravitational force factor employable raises the combined operating range of the throughputs in addition to their flexibility due to the additional degree of freedom offered by the rotation speed [3].

A fundamental aspect of the modelling, design, optimization, and implementation of pilot-scale and subsequent scale-up of RPB reactors is the clear understanding of the principles of its hydrodynamics via accurate prediction of the pressure drops and upper operating limits [3], [4]. Also, Zhang et al. [6] observed that the mass transfer performance and efficiency of an RPB reactor, as reflected by its gas pressure drop, is closely linked to its hydrodynamic characteristics, operating costs, and energy requirements. Hydrodynamic characteristics such as

the pressure drop of an RPB reactor are a useful index in measuring its resistance and consequent energy consumption [7]. Many studies were carried out to evaluate the influence of pressure drop in many RPB reactor operations with empirical and semi-empirical models established [8], [9]. RPB reactor hydrodynamic parameters extensively reported in the literature include liquid holdup [10], [11], gas pressure drop (Neumann et al., 2017b; Pyka et al., 2022), liquid dispersion [11], [14] and, flooding [4], [15]. Although extensive research has been conducted and documented using RPB reactors, with many of its applications explored at the industrial scale, its design approach is still case-specific. It thus requires improvements (Neumann, et al., 2017a).

Cortes et al. [17] reviewed various advantages and disadvantages of RPB reactors regarding its mass-transfer performance, hydrodynamic behaviour, as well as the complexity and suitability of the rotor to be filled with catalyst packing for the purpose of heterogeneous reactions. The relatively high rotation speeds of RPB reactors combined with the size of the equipment make it possible to implement forces more than 100 times greater than gravity, greatly intensifying the transfer phenomena between phases [18]. Rapid contact surface replacement in RPB reactors allows for high effective surface area packings of 2000 to 5000m^2/m^3 [18]. This allows for higher mass transfer characteristics: gas-liquid interfacial area, gas-side and liquid-side volumetric mass transfer coefficients, and height of transfer unit (Cheng & Tan, 2011; Zhang et al., 2011). Also, this allows for the same separation performance in RPB reactor to have much more flexible and compact equipment with a wider operating range than a gravity column used for absorption [19]. Overall, compared to conventional gravity columns, for a comparable processing capacity and efficiency, a RPB reactor offers rotation as an extra degree of freedom, serves as the foundation of modular plants, and is more miniaturized with higher flexibility and energy efficiency [21]. The characteristics mentioned above make RPB reactors emblematic equipment for process intensification. Consequently, RPB reactors have been employed for various purposes in diverse fields such as separation processes, synthesis, and preparation of micro and nano-particles, petroleum products processing, biodiesel production, medical sciences, and pollution control [2], [19], [21].

Results of preliminarily studies involving liquid–solid processes conducted by [22], [23] and [24] revealed that the apparent reaction rates of heterogeneous catalytic reactions can be increased 33–39 times when conducted in RPB reactor reactors compared to when conducted in conventional packed bed reactors. In their study, Chang et al. [22], used RPB reactor as a catalytic ozonation reactor for the decomposition of phenol and reported that the process efficiency was influenced by the rotation speed, catalyst packing mass, UV irradiation intensity, ozone gas flow rate and temperature. The modelling of the integration of simultaneous reaction and stripping for an esterification reaction was achieved in a solid catalyzed reactive RPB stripper was reported by Gudena et al. [23]. At a rotation speed of at 1000 rpm, the results, showed a 56% enhancement in concentration of produced octyl-hexanoate ester and a 30% rise in ester concentration when the RPB stripper was used as compared to when traditional reactors are used. Also, the dissolution of copper by potassium dichromate to study the liquid–solid mass transfer in a RPB reactor equipped with a structured foam packing was use to lay the foundation for the modelling of RPB reactors for heterogeneous catalytic reaction by Liu et al. [25]. The liquid–solid volumetric mass transfer coefficient was found to be in the range 0.04–0.14 s^{-1}, and was about 500% higher than what was obtained with a conventional packed bed reactor. The findings above as reported in [21] - [24] attests to the potentials of the RPB reactor for multi-phase catalytic reactions. However, Liu et al. [25] observed that the paucity of the fundamental understanding and data on the complex liquid–solid mass transfer in RPB reactors is a limitation to its design and scale-up. Hence, the need for more fundamental studies on the RPB reactor.

A sketch of a conventional, single-stage RPB reactor as presented by Garba et al. [26] is shown in Figure 1. It comprises of a casing surrounding a rotor mounted on a shaft and rotated by a motor. The rotor is a motor-driven, ring-shaped cylinder that encloses an annular packing mounted on either a horizontal or a vertical shaft. In countercurrent operation mode, gas is introduced into the outer periphery of the packing from the casing. The liquid is usually introduced into the center (or “eye”) of the rotor via the liquid inlet through a stationary set of nozzles (liquid distributor) into the packing from the top of the RPB. After its transformation by centrifugal shear forces, the liquid flows in the form of rivulets, droplets, or films as determined by the rotation speed [10]. The casing wall finally collects it and flows downwards under gravity, leaving the casing via the liquid outlet.

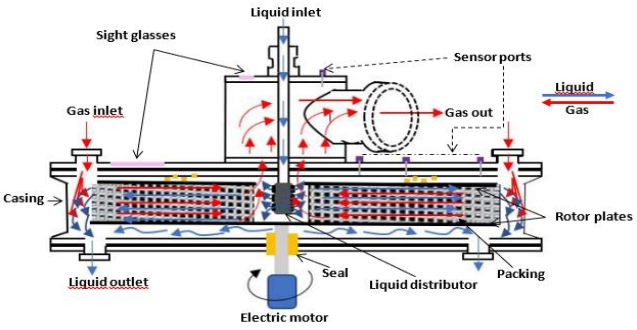

Figure 1. Schematic of a countercurrent flow RPB reactor [26]

As equipment for efficient multi-phase mixing and mass transfer, [27] identified RPB packing as its core component. Because of its excellent mass transfer characteristics, stainless steel wire mesh is commonly used as RPB packing [28]. For catalyzed reactions, in addition to the ease in catalysts loading, the high centrifugal force field

in RPB reactors, has necessitated the use of structured as opposed to pellet catalysts to prevent squeezing and possible crushing of the catalysts. Also, the use of structured catalysts packing can overcome the cumbersome step of bulk catalysts loading [24].

Conventional separation packed beds have constant cross-sections. Thus, their packing pores are nearly wholly filled throughout the column during flooding, causing a noticeable, steep rise in pressure drop. However, due to the rotor geometry, RPB reactor packings have variable cross-sections. The centrifugal forces are lowest at the center (eye) of the rotor. Hence, RPB reactor flooding occurs in the eye from where the liquid is ejected. Consequently, pressure drop variations during flooding in RPB reactors are not consistent as the sole indicator of flooding. (Neumann et al., 2017a), and Lockett [15] also reported that in contrast to conventional columns, for RPB reactors, no sharp inflection in the total pressure drop or the holdup of the liquid with the gas velocity was observed during flooding. The procedure for visually determining the upper operating limit is to neutralize two operating variables and manipulate the third one [3]. Therefore, it is possible to carry out two procedures to reconfirm the results. The speed of the rotor and the liquid flow rate may be set to a constant value then the gas flow rate gradually increases until an excessive splash of the liquid is observed in the eye of the rotor. Allowing the gas flow rate to increase beyond the upper operating limit will cause the liquid to accumulate in the eye of the rotor. (Groß et al., 2018; Neumann et al., 2017b) recommended the use of a combination of visual and quantitative approaches to adequately study the flow behavior in RPB reactors, while [3] observed that due to observed inconsistencies, the use of physical and visual observations and the measurement of pressure drop variations alone are not sufficiently adequate to predict flooding behavior in RPB reactors. [10] used liquid holdup, while [4] measured the flow rate of entrained liquid from the eye of the rotor to identify the upper operating limits in RPB reactors.

This work presents a robust quantitative method of obtaining RPB reactor upper operating limit based on the flow rate of the ejected liquid, supported by visual observation and pressure drop measurements. This was achieved by connecting a hydrocyclone to the gas outlet. In addition, a comprehensive pressure drop behavior and flooding for a countercurrent water-air system and a single-block stainless steel wire mesh packing using a double jet nozzle for the liquid inlet were used to study the hydrodynamics of the pilot-scale RPB reactor. The aim was to improve further the understanding of RPB reactor hydrodynamics for design, scale-up, and energy conservation purposes.

2. EXPERIMENTS

The experimental setup is shown in Figure 2. The RPB reactor was a commercial pilot-scale RPB reactor 500 supplied by ProCeller®, Poland. The RPB reactor was a single-stage, vertical rotor type with a casing diameter of 0.676m, an inner rotor diameter of 0.160m, and an outer rotor diameter of 0.500m. The packing was supplied along with the RPB reactor reactor and it was a conventional, multi-layered, single-block, stainless steel wire mesh with an axial height of 0.040m, a specific surface of 2400 m^2/m^3, and a porosity of 86%. Visual observation was possible using two inspection glasses placed directly above the eye of the rotor and another on the casing (Figure 3a). To aid the systematic collection and subsequent measurement of ejected water from the eye of the rotor during flooding, a hydrocyclone was connected to the gas outlet. A countercurrent air-water system was used for all the experiments. The rotation speed of the rotor was selected and auto-controlled via a variable frequency drive. The liquid was pumped to the RPB reactor using a peristaltic pump and controlled with a valve.

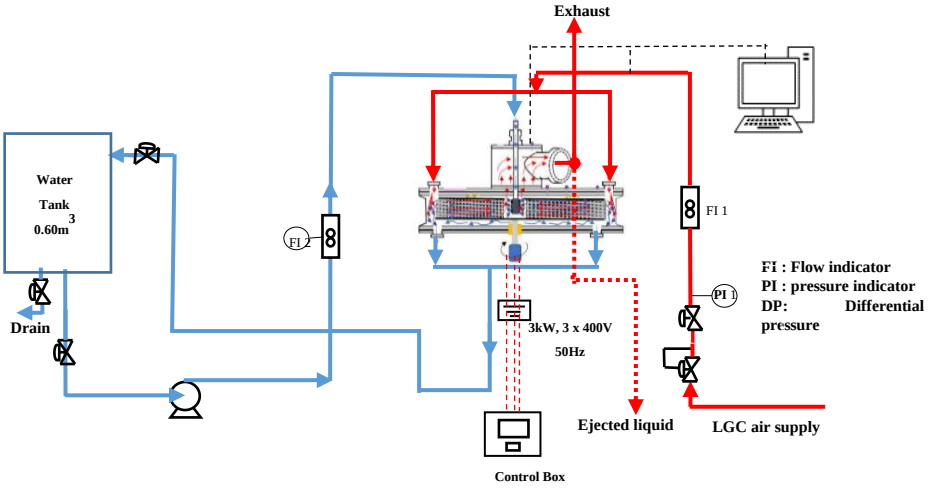

Figure 2. Countercurrent process flow diagram of the RPB reactor

The liquid flow rate was measured with a panel-type rotameter and sprayed from the center of the RPB reactor using a dual nozzle, flat fan liquid distributor. The liquid was recirculated to the feed tank using a bypass line. An air supply from the general laboratory compressor was used. The gas was introduced into the outside of the RPB reactor into the casing through twin gas inlets and leaves after passing through the packing via the gas outlet. While the liquid sprays outwards from the center of the packing to its periphery. A pressure sensor connected to a pressure transmitter was placed across the two points to measure the pressure drop between the packing periphery and the gas outlet. Pressure drop was measured in real time by interfacing the sensor to a computer using a data acquisition system.

The range of operating parameters studied was: gas flow rate (V_G), 0-400Nm^3/h; liquid flow rate (V_L), 0-0.84m^3/h and rotation speed 0-1500 revolutions per minute (RPM). Each experimental run was for 5 minutes. In the dry pressure drop measurements, the frictional pressure drop was first measured by passing air at 100Nm^3/h through the stationary rotor and then measuring the pressure drop. The experiment was repeated by increasing the airflow rate in steps of 50Nm^3/h. The same procedure was repeated with the rotor at various rotation speeds. Next, the effect of the rotation speed was investigated, initially via the centrifugal pressure drop. Without liquid and gas flow, the rotor was set to an initial speed of 100 rpm. The rotation speed was subsequently changed stepwise. The effect of rotation speed was further investigated by varying the rotation speed at constant gas flow rates. For the wet pressure drop, rotation speeds and liquid flow rates were kept while the gas flow rate was increased stepwise. This was followed by another set of experiments during which the gas flow rate and rotation speed were kept constant while the liquid flow rate was increased. The liquid flow rate and rotation speed were kept constant to determine the upper operating limit. In contrast, the gas flow rate was increased stepwise until the first drops of water were observed from the gas outlet according to the arrangement shown in Figure 3e. This point was taken as the upper operating limit of the RPB reactor at the prevailing combination of operating factors. The reduction in rotation speed was continued gradually, with the amount of ejected water measured at each step after attaining a steady state of operation. Flooding points of the RPB reactor operations were determined by visual observation of excessive water splashing at the RPB reactor eye, with or without a sharp increase in pressure drop. The volume of water ejected at each step change of the gas flowrate was collected and measured using a measuring cylinder, and the flooding point was taken following the recommendation of [4] when the flow rate of the ejected liquid is the same or exceeds 8 % of the liquid flow rate.

3. RESULTS AND DISCUSSION

3.1 Effect of operating parameters on the single-phase pressure drops

Figure 3 shows the influence of the gas flow rate and the rotation speed on the single phase (dry) pressure drop. Figure 3 (a) shows the dry pressure drop increases with increase in rotation speed. A slow increase in the pressure drop was obtained at low rotational speeds from 100 to 550 rpm. Above 600 rpm, a rapid and almost linear increase in pressure drop was obtained. This phenomenon may be due to the greater need to overcome the pressure drop caused by rotation (centrifugal head) at higher rotational speeds, which consequently causes the air in the rotor and between it and the casing to rotate. The dry bed average increase in pressure drops per unit increase in rotation speed in the range investigated was 0.75Pa/rpm. This shows that centrifugal pressure contributes significantly to the total dry-packing pressure drop. Figure 3(b) shows a substantially linear increase in pressure drop with increasing gas flow rate. The effects of gas inertia and friction primarily cause this. On average, Figure 3(b) shows that the average increase in pressure drop per unit increase in gas flow rate was 4.11Pa/Nm^3h^{-1} within the operating range investigated.

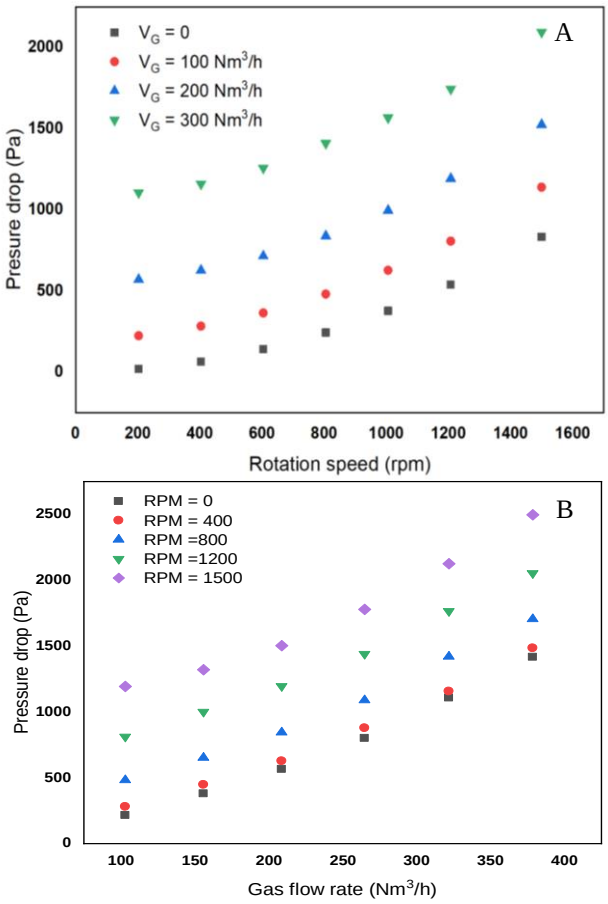

Figure 3. Dry bed pressure drops (A) effect of rotation speed (B) effect of gas flowrate

3.2 Effect of operating parameters on the total pressure drop

For the irrigated bed, Figures 4(a) and (b), shows that the trend of the pressure drop variation was similar to that of the dry bed, with the pressure drop increasing with an increase in rotational speed and with the gas flow. [5] identified the wetting of the packing surface, which affects the frictional pressure drop, and the blockage of the packing pores by the liquid to the passage of gas as the two principal contributors to the rise in pressure drop in wet RPB reactors.

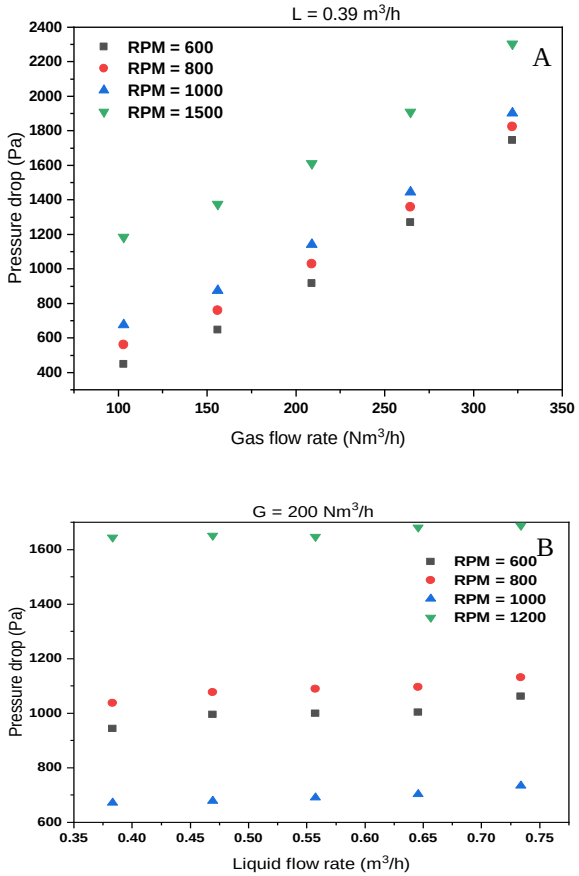

Figure 4. Wet bed pressure drops (A) effect of gas flowrate (B) effect of liquid flowrate

Figure 4(b) indicates the lower effect of liquid flow rate on the overall pressure drop in RPB reactors. For example, for a gas flow of 350Nm^3/h, the 50% increase in liquid flow rate from 0.3 to 0.6 m^3/h produces small changes in the pressure drop with the increase in the speed of rotation, showing that the effect of the gas flow in the RPB reactor is more than that of the liquid flows. The average unit increase of 5.73Pa/Nm^3/h for a fixed liquid flow rate of 0.39 m^3/h indicates the higher pressure drop due to the presence of the liquid as opposed to the 4.11 Pa/Nm^3/h. This phenomenon is more visible when we represent this at constant rotational speeds with a variation of the gas flow (Figure 4a) or a variation of the liquid flow (Figure 4(b). These results confirm the trends described by the reports of [3], [16]. Additionally, in terms of liquid loading loads and gas capacities, it can be deduced that the ranges of the wet pressure drops in Figures 5(a) and (b) are comparable to the findings of [7].

3.3 The upper operating limit of the RPB reactor

Figure 5 (a) shows that the flooding data follows a typical RPB reactor equipped with a vertical axis pressure drop variation curve with rotation speed at constant gas and liquid flow rates, as highlighted by [16]. A lowering of centrifugal pressure drop is obtained at a decrease from the maximum rotation speeds. At the same time, liquid accumulation in the eye causes only slight increases in frictional pressure drop. Further decrease in the rotation speed will cause an accumulation of liquid in the eye of the rotor, which leads to an increase in the frictional pressure drop and a sharp increase in the total pressure drop.

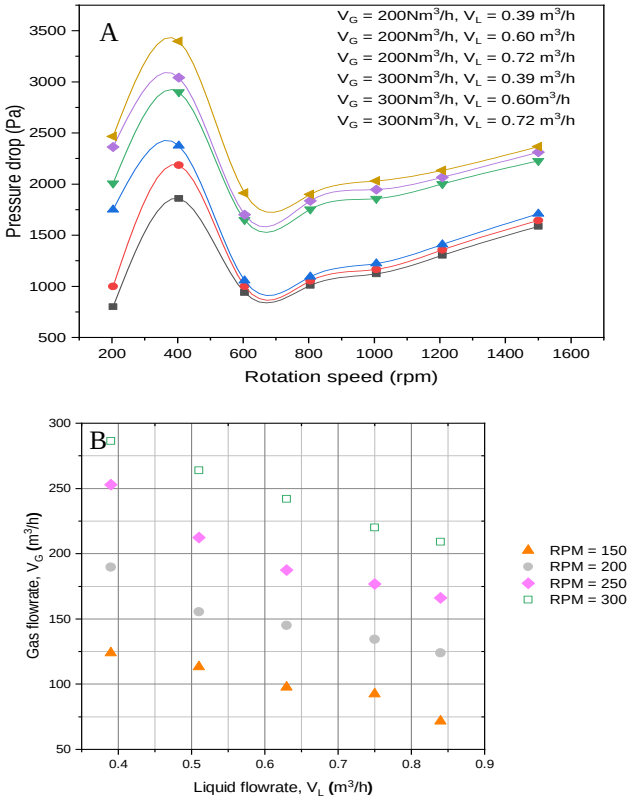

Figure 5. (A) Effect of rotation speed at constant gas and liquid flow rates (B) upper operating points

As the rotation speed is further decreased, rapid ejection of liquid from the eye of the rotor to the gas outlet is obtained due to the acceleration of the liquid droplets. The pressure drop increases significantly, and the presence of water is visually observable in the rotor eye. Figure 5(b) shows the upper operating limits of the system investigated. At a constant rotation speed, the gas flow rate at which the ejection of liquid droplets was observed and decreased with an increased liquid flow rate. Regular operation of the RPB reactor without liquid ejection and possible high-pressure drops, which increase power consumption, is obtained by operating the RPB reactor below the indicated points. The

operating limit at a given condition can be improved by increasing the rotation speed from the given point. Based on a range of liquid loads and the gas capacity factor at the inner radius of the RPB reactor, the trends and ranges of these operating limits are comparable to the results of [3].

4. CONCLUSION

This paper focused on furthering the understanding of the fundamentals of the RPB reactor as an intensified reactor for enhancing heterogeneous catalytic reactions. The barrier imposed by the lack of fundamental data on the design modelling and scale-up of RPB reactor reactors was bridged by the presenting hydrodynamic characteristic data necessary for the evaluation of the mass transfer processes. Hence, the gas pressure drops of a pilot-scale RPB reactor equipped with stainless steel wire mesh packing for an air-water system using a twin-nozzle liquid distributor was explored. A robust approach to determine RPB reactor operating limits based on quantifying the volume of liquid ejected from the eye of the rotor was explored. Low rotational speeds from 100 to 550 RPM generate slow increase in pressure drop while rotation speeds above 600 rpm generated rapid and almost linear increase in pressure drop. The trends were attributed to the higher need to overcome the centrifugal head caused by rotation at higher rotational speeds which forces the rotation of the gas entrapped in the reactor. Within the range of operating conditions investigated, the average increase in pressure drop per unit increase in rotation speed was 0.75Pa/rpm. The operating limits for RPB reactor are influenced mainly by the three operational parameters: gas flow rate, liquid flow rate, and rotational speed in that order.

ACKNOWLEDGEMENTS

This work was conducted under support funding from the Overseas Scholarship Scheme (OSS) of the Petroleum Technology Development Fund (PTDF), Nigeria (Grant Number: PTDF/ED/OSS/PHD/UG/1543/19).

REFERENCES

1. Adekola Lawal, O. O., Meihong, W., Peter, S., Fuel, **101** (2012) 115–128.
2. Hilpert, M., and Repke, J. U., Ind. Eng. Chem. Res, **60** (2021) 5251–5263. doi: 10.1021/acs.iecr.1c00440.
3. Groß, K., Neumann, K., Skiborowski, M., and Górak, A., Chem. Eng. Trans. **69** (2018) 661–666. doi: 10.3303/CET1869111.
4. Hendry, J. R., Lee, J. G. M., and Attidekou, P. S., Chem. Eng. Process. - Process Intensif. **151** (2020) 107908. doi: 10.1016/j.cep.2020.107908.
5. Zhang, W., Xie, P., Li, Y.L., Teng, and Zhu, J., J. Nat. Gas Sci. Eng. **79** (2020) 103373. doi: 10.1016/j.jngse.2020.103373.
6. Wen, Z. N., Wu, W., Luo, Y.,. Zhang, L. L., Sun, B. C., and Chu, G. W., Ind. Eng. Chem. Res. **59** (2020) 16043–16051. doi: 10.1021/acs.iecr.0c01886.
7. Liu, X., Jing, M., Chen, S., and Du, L., Can. J. Chem. Eng. **96** (2018) 90–596. doi: 10.1002/cjce.22936.
8. Singh, S. P. et al., Ind. Eng. Chem. Res. **31** (1992) 574–580. doi: 10.1021/ie00002a019.
9. Jiao, W. Z., Liu, Y. Z., and Qi, G. S., Ind. Eng. Chem. Res. **49** (2010) 3732–3740. doi: 10.1021/ie9009777.
10. Burns, J. R., Jamil, J. N., and Ramshaw, C., Chem. Eng. Sci. **55** (2000) 2401–2415. doi: 10.1016/S0009-2509(99)00520-5.
11. Burns, J. R. and Ramshaw, C., Chem. Eng. Sci. **51** (1996) 1347–1352. doi: 10.1016/0009-2509(95)00367-3.
12. Pyka, T. J., Koop, C. Held, and G. Schembecker, Ind. Eng. Chem. Res. (2022). doi: 10.1021/acs.iecr.2c02500.
13. Neumann, K., Hunold, S., Skiborowski, M., and Górak, A., Ind. Eng. Chem. Res. **56** (2017) 12395–12405. doi: 10.1021/acs.iecr.7b03203.
14. Xie, P. (2019).
15. Lockett, M. J., Chem. Eng. Res. Des. **73** (1995) 379–384.
16. Neumann, K., Hunold, S., Groß, K., and Górak, A., Chem. Eng. Process. Process Intensif., **121** (2017) 240–247. doi: 10.1016/j.cep.2017.09.003.
17. Cortes Garcia, G. E., van der Schaaf, J., and Kiss, A. A. J. Chem. Technol. Biotechnol. 92 (2017) 1136–1156. doi: 10.1002/jctb.5206.
18. Pan, S. Y., Wang, P., Chen, Q., Jiang, W. Y. H., and Chiang, P. C., J. Clean. Prod. 149 (2017) 540–556. doi: 10.1016/j.jclepro.2017.02.108.
19. Zhang, L. L., Wang, J. X., Xiang, Y., Zeng, X. F., and Chen, J. F., Ind. Eng. Chem. Res. 50 (2011) 6957–6964. doi: 10.1021/ie1025979.
20. Cheng, H. H., and Tan, C. S., Sep. Purif. Technol. **82** (2011) 156–166. doi: 10.1016/j.seppur.2011.09.004.
21. Neumann, K., et al., Chem. Eng. Res. Des. **134** (2018) 443–462. doi: 10.1016/j.cherd.2018.04.024.
22. Chang, C., Chiu, C., Chang, C., and Chang, C., J Hazmat. **168** (2009) 49–55. doi: 10.1016/j.jhazmat.2009.02.171.
23. Gudena Krishna, G. P. R., Tay Haw Min, Chem. Eng. Sci. **80** (2012) 242-252.
24. Liu, Y., Li, Z., Chu, G., Shao, L., Luo, Y., and Chen, J., Chinese J. Chem. Eng. **28** (2020) 2507–2512. doi: 10.1016/j.cjche.2020.06.038.
25. Ya-zhao Liu, J. C., Li, Z., Chu, G., Shao, L., Luo. Y., Chinese J. Chem Eng. **28** (2020) 2507–2512.
26. Garba, U., Rouzineau, D., and Meyer, M., MATEC Web Conf. **04003** (2023) 1–8, [Online]. Available: https://doi.org/10.1051/matecconf/202337904003

27. Yuan, Z.-G., Wang, Y.-X., Liu, Y.-Z., Wang, D., Jiao, W.-Z., andLiang, P.-F., Chinese J. Chem. Eng. **49** (2021) 178–186. doi: 10.1016/j.cjche.2021.12.023.
28. Chen, Y. S., Lin, F. Y., Lin, C. C., Der Tai, C. Y., and Liu, H. S., Ind. Eng. Chem. Res. **45** (2006) 6846–6853. doi: 10.1021/ie060399l.